J Mater Sci (2009) 44:408–413
DOI 10.1007/s10853-008-3131-y

The variation of beta phase morphology after creep and negative creep for duplex titanium alloys

Shing-Hoa Wang · Hao-Hsun Lee · Chih-Yuan Chen · Jer-Ren Yang · Chin-Hai Kao

Received: 19 April 2008 / Accepted: 24 November 2008 / Published online: 11 December 2008
© Springer Science+Business Media, LLC 2008

Abstract The creep resistance of SP700 (Ti–4.5Al–3V–2Mo–2Fe) is superior to Ti–6–4 (Ti–6Al–4V) at 500 °C under a constant load corresponding to an initial stress of 100 MPa. The β phase grains in the SP700 alloy prefer to orient along the loading axis in contrast to the Ti–6–4 alloy. The grain growth occurs during the stress drop incubation period. The observation of different amounts of negative creep/anelasticity upon loading is closely associated with the difference in the amount of grain/subgrain coarsening.

Introduction

Titanium alloys are classified as structural materials due to their high strength, good fatigue properties, superplasticity formation, and light weight. They are mostly used in the aerospace industry due to their good fatigue life and as biological materials due to their excellent biocompatibility. Titanium alloys are also excellent for applications in structural components submitted to high temperatures [1]. However, because of surface oxidation, titanium alloys are limited to use at temperatures below 600 °C. Of all the titanium alloys, the $\alpha + \beta$ duplex phase titanium alloys are the one most commonly used, especially Ti–6–4 (Ti–6Al–4V), whose optimum balance of properties have made it by far the most popular titanium alloy. Under different heat treatments, Ti–6–4 develops different volume fractions of the two phases and different microstructures. For example, Ti–6–4 has an α phase of 90% if the cooling rate is very low, but with increased cooling rates, the microstructure reveals three types of structures: lamellar, equiaxed, and bimodal type microstructures [2]. Another $\alpha + \beta$ titanium alloy, SP700 (Ti–4.5Al–3V–2Mo–2Fe), has been developed with a lower superplasticity forming temperature of 750 °C, relatively lower than that of Ti–6–4, which has a superplasticity temperature of 900 °C. SP700 is classified as a β-rich $\alpha + \beta$ titanium alloy. The Mo addition in SP700 is characterized as a β stabilized element and makes the β transus (900 °C) of SP700 lower than of Ti–6–4 (978 °C) [3]. At room temperature, duplex titanium alloy SP700 rich in β phase has increased workability, and the fine structure promotes the mechanical properties and superplasticity. The acicular α phase precipitate in the β phase for SP700 alloy at 830 °C tends to coarsen from fine to coarse with increased annealing temperature. The volume fraction and grain size of the α and β phases also change with annealing temperature. Both the volume fraction and grain size of the β phase increase with annealing temperature, resulting in a decrease in α phase [4].

Because of the lower superplasticity forming temperature and the addition of Mo, which has less diffusivity, the grain growth is limited during superplasticity forming [5]. At the superplastic forming temperature with a fine grain size 2.3 μm and 70% volume fraction of β phase, the elongation of SP700 alloy can attain 2,500%, which is much higher than that of Ti–6–4. The addition of Mo can inhibit the grain growth under high temperature

S.-H. Wang (✉) · H.-H. Lee
Department of Mechanical Engineering, National Taiwan Ocean University, 20224 Keelung, Taiwan
e-mail: shwang@ntou.edu.tw

C.-Y. Chen · J.-R. Yang
Institute of Materials Science and Engineering, National Taiwan University, 10617 Taipei, Taiwan

C.-H. Kao
S-Tech Corporation, Sinying 730, Tainan, Taiwan

deformation [6]. The features of very fine microstructure, low β transus temperature, low flow stress, and suppressed grain growth all make SP700 alloy suitable for real superplastic forming in several applications.

The creep behavior of Ti–6–4 was investigated under constant load in a stress range from 291 to 520 MPa at 500 °C and from 97 to 319 MPa at 600 °C. Ti–6–4 was controlled by dislocation climb in the hexagonal α phase [7]. The increase in tertiary creep rate was related to the necking development and to nucleation and coalescence of microvoids [7]. Seco [8] also showed that the temperature activated dislocation climb was the mechanism responsible for the failure of Ti–6–4 thick plate, which under the β-annealed condition (1,030 °C for 30 min, air cooled and aged for 2 h at 730 °C) can have the maximum times to failure. The fracture surfaces of these broken specimens exhibited an intergranular morphology which was attributed to grain boundaries sliding along the former β grains. Primary creep behavior was studied in Ti–6–22–22S (Ti–6Al–2Sn–2Zr–2Cr–2Mo–0.16Si) alloy under 480 °C and stress range from 150 MPa to 500 MPa [9]. Ti–6–22–22S, $\alpha + \beta$ duplex phase titanium alloy, was compared with other Ti alloys by analyzing the Larson-Miller time to reach 0.1% creep strain. Alloy Ti–6–22–22S has a much larger Larson-Miller parameter than Ti–6–4, because the creep resistance of the former is better than that of the latter.

There is no literature on the creep of β-rich SP700, especially in the aspect of stress drop creep. This study characterizes the behavior and microstructure of Ti–6–4 and β-rich SP700 under the same test conditions. Here, the behavior of the steady state creep and the subsequent stress drop creep are compared, and their variations in microstructure arrangement are observed.

Experimental procedure

Titanium alloy Ti–6–4 was hot rolled into a round bar of 13 mm in diameter at 950 °C and annealing at 730 °C, followed by air cooling. Another SP700 titanium alloy was made with the same manufacturing process as that of Ti–6–4, but with the rolling temperature at 800 °C and annealing at 718 °C. The constant load tensile creep tests and drop test were conducted in air under an initial stress of 100 MPa at a temperature of 500 °C for 160 h. The creep strain was measured by using a super linear variable capacitor (SLVC). In another test, after steady state creeping for 140 h, the stress was unloaded and reduced to 30% of the initial stress. Then the specimens were allowed to continue creeping at a low stress level of 30 MPa for about 20 h, so that the creep strain change could be observed.

The average composition of both materials, determined by energy dispersive spectrometry (EDS), is given in Table 1. The optical microstructure of mechanical polished specimens was etched with a solution composed of 10% HF, 5% nitric acid and 85% water for 5 s. The α phase (hexagonal closed pack, hcp) and β phase (body center cubic, bcc) were identified using a Hitachi S4100 scanning electron microscope (SEM) with an energy dispersive spectrometer (EDS) attached. The crept specimens within the gage length for transmission electron microscopy (TEM) were twin-jet electron-polished with a solution composed of 5% sulfuric acid and 95% methanol.

Table 1 Chemical composition analysis by EDS (wt%)

Materials	Ti	Al	V	Fe	Mo	O	N	H
Ti–6–4	Bal.	6.25	3.8	0.3	–	0.16	0.01	0.006
SP700	Bal.	4.2	2.8	2.1	2.0	0.12	0.02	0.004

Results and discussion

Typical microstructures of the as-received Ti–6–4 and SP700 after hot rolling and annealing are shown in Fig. 1a, b. EDS confirmed that the brightly imaging grains can be attributed to the β phases. The grain sizes of this phase are about 0.5 μm for Ti–6–4 and about 1.2 μm for SP700, respectively. The magnitude of grain size for both alloys agrees with the literature reported [10] in the fine grain range. Both titanium alloys show white β phase islands that may be the result of the continuous β phase being broken into isolated pieces by the duplex annealing treatment [11].

Both titanium alloys, α-rich Ti–6–4 and β-rich SP700, exhibit a typical creep curve consisting of well-defined primary and secondary stages, as shown in Fig. 2a. The primary creep stage of SP700 lasted about 25 h, but that of Ti–6–4 lasted only 20 h. During this period, the material was hardening most probably due to the accumulation of dislocations. After the primary creep, both titanium alloys crept at steady state for about 140 h. The minimum creep rate of Ti–6–4, with less β phase, was 3×10^{-4}/h, which is about three times higher than that of β-rich SP700, at 1×10^{-4}/h. The relatively equiaxed beta grains exist in both as-received duplex titanium alloys. In the steady creep case, the beta grains are coarsened in Ti–6–4(Fig. 1c), but they are elongated and oriented with the tensile loading direction in addition to the coarsening in SP700 (Fig. 1d). Thus the high temperature creep resistance of SP700 is superior to that of Ti–6–4 and is attributed to the large and deformed elongated β grains in the former alloy. The creep deformation of the duplex phase of Ti–6–4 is mainly dominated by dislocation climb in the alpha phase in a stress range from 291 to 520 MPa at 500 °C and in a stress range from 97 to 319 MPa at 600 °C [12]. In contrast, the creep of

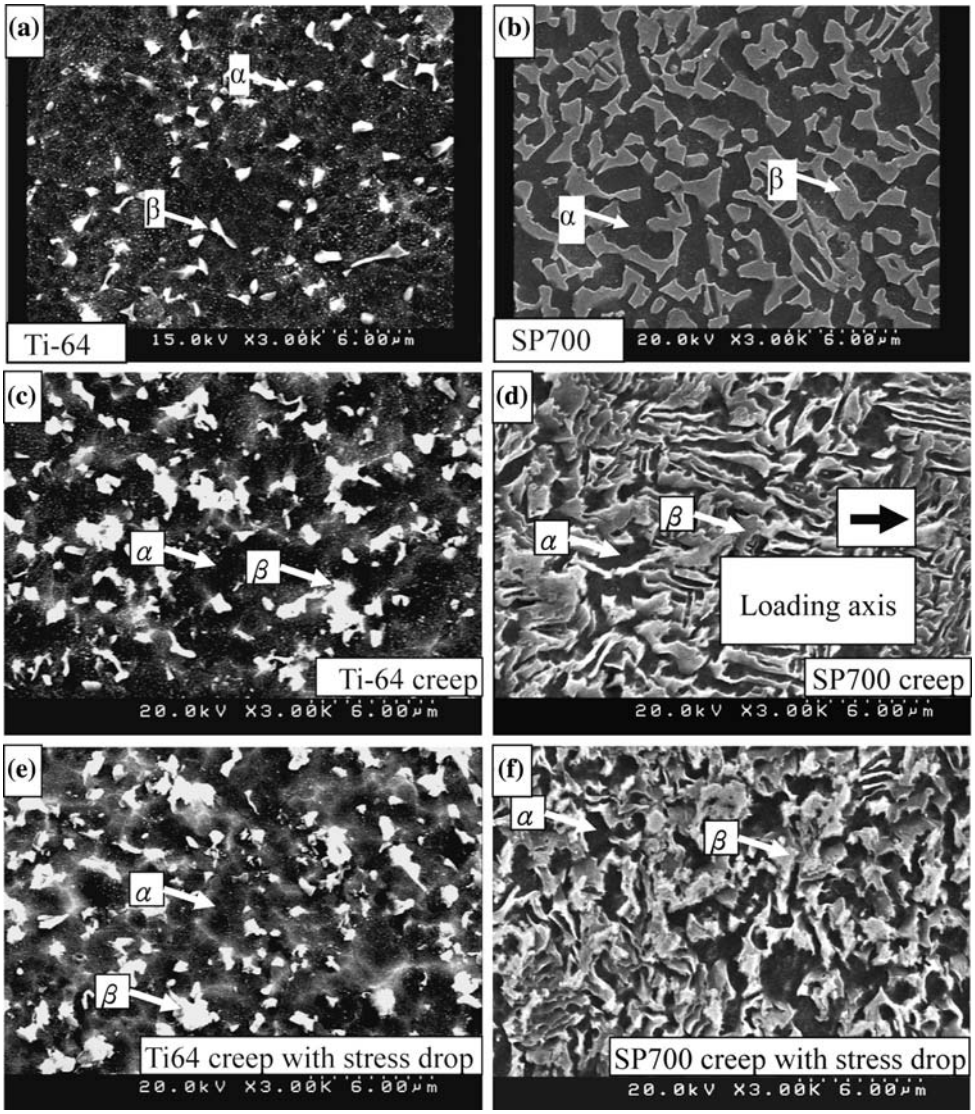

Fig. 1 The SEM micrograph of Ti–6–4 and SP700 alloys **a** and **b** as-received; **c** and **d** 160 h creep; **e** and **f** 140 h creep followed by negative creep 20 h after the stress drop

the SP700 titanium alloy is dominated by the deformation of the β phase which is the major phase in this alloy.

The creep stress drop was carried out when the specimen had crept for 140 h, and it was followed by 20 h of low stress creep, as shown in Fig. 2b. At constant creep, the steady state at the stage of a dynamic balance exists between strain hardening and recovery. It follows that the level of the internal stress is independent of time. Kruml [13] mentioned that the applied stress on a material is often assumed to be separated into two distinct parts, effective stress and internal stress. The effective stress is supposed to depend on temperature and plastic strain-rate. The mechanical properties of the material are strongly dependent on both the microstructure and the test environment. The total internal stress is a complex superposition of phenomena caused by dislocation tangles, cell structures, solute-dislocation interactions, precipitate particles, subgrains, dislocation pileups, and bowing of pinned dislocations between their obstacles [12]. A theory of the relation between the effective stress, internal stress, and stress reduction has been proposed by Ahlquist and Nix [14]. They suggested that, if the creep rate is negative, the internal stress is larger than the new stress ($\sigma - \Delta\sigma < \sigma_i$). After the decrease of the applied stress by $\Delta\sigma$, instantaneous contraction appears. The contraction is due to the elastic strain at high temperature, depending on the temperature and high temperature properties of the material. There is no doubt in Fig. 2b that the sudden reverse elastic strain corresponding to the stress drop $\Delta\sigma$ is apparent. After the decrease of the elastic strain, the curve follows a reverse creep course [15], depending on the time for the structure relaxation. The trend of the transition creep curves for both titanium alloys exhibits a negative creep rate [15]. Under the same magnitude of unloading, the elastic recovery of SP700 is clearly larger, and negative creep rate is one-fifth of that of Ti–6–4 in Fig. 3. This is

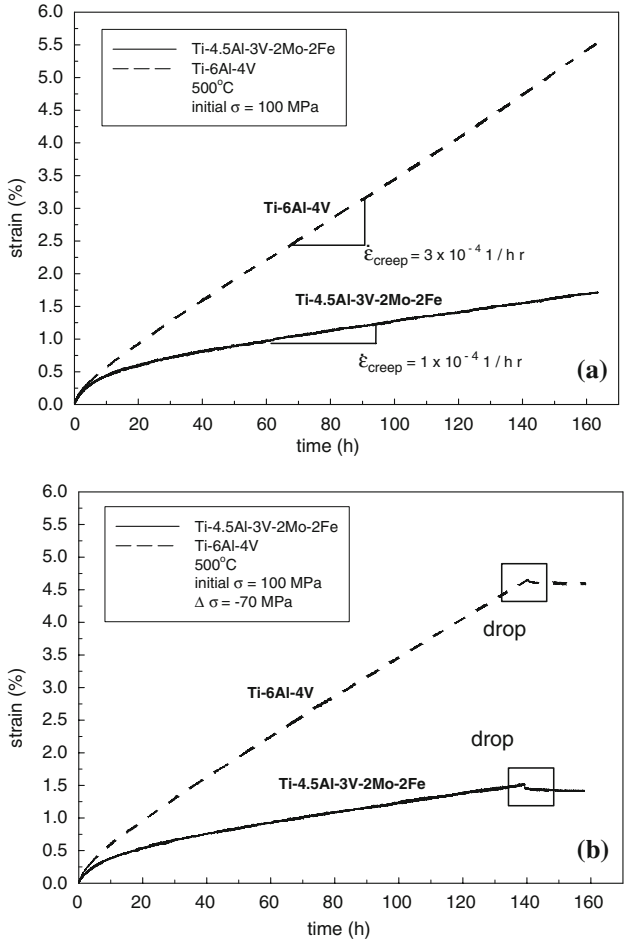

Fig. 2 **a** The creep curves of alloys at 500 °C for 160 h. **b** The creep curves of alloys at 500 °C for 140 h followed by negative creep 20 h after a sudden 70 MPa stress drop

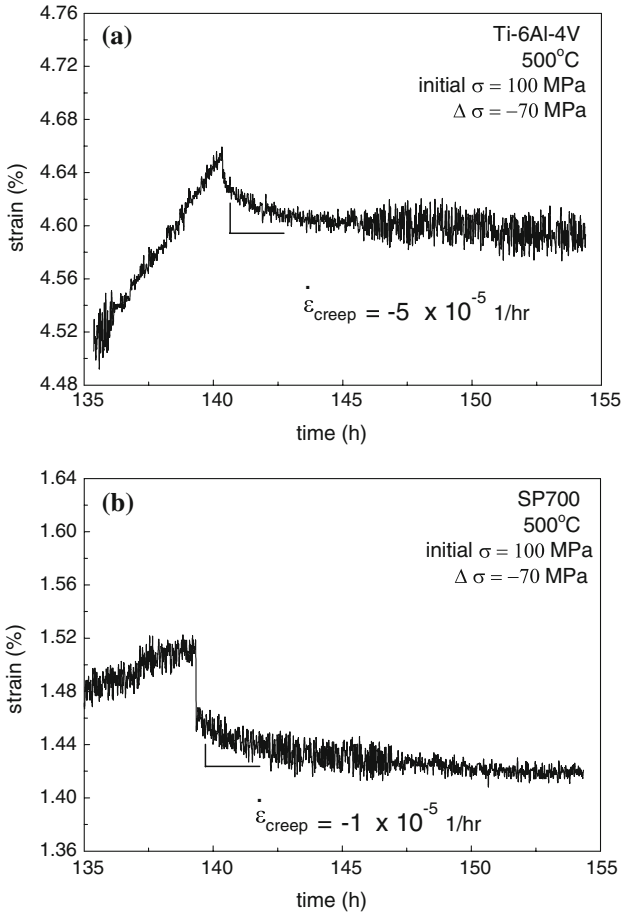

Fig. 3 The enlarged creep curve of an inserted square frame in Fig. 2 for **a** Ti–6–4 alloy and **b** SP700 alloy

due to the former having a higher internal stress and a low amount of grain coarsening, as discussed in a later section. This phenomenon is similar to the stress drop creep of Al–Mg alloys [14] and is near that of the α Timetal 834 titanium alloy [16]. The response of negative creep after stress drop for Ti–6–4 and SP700 in Fig. 2 indicates that the internal stress is larger than the new stress level ($\sigma - \Delta\sigma$). In other words, the new stress level is smaller than the effective stress for both titanium alloys. The internal stress is a result of the dynamic balance between strain hardening and recovery. One expects internal stress to change when the applied stress and temperature change; in addition, the effective stress is responsible for glide [12]. The zero creep rates of Ti–6–4 and SP700 begin to occur 3 h after the stress drop. At this stage, the recovery of the structure occurs, allowing creep to proceed once the internal stress has been lowered to the level of the reduced stress [17]. It is suggested that if the incubation continues for longer hours, the new steady state creep at the reduced stress level will be triggered again. The new creep rate depends on the difference between the applied stress and the mean internal stress [12]. The state of the internal stress is generally regarded as a characteristic of resistance of structure against dislocation motion.

During the 20-hour period of negative creep following the stress drop, the beta grains tend to become randomly distributed and develop an equiaxed morphology (Fig. 1e, f) apparently driven by the interface tension effect. Therefore, the material softens during this period. To further understand the behavior of creep and creep with stress drop in Fig. 2 for both Ti–6–4 and SP700, the structure variations were examined with the TEM. Dislocation creep involves three stages: (i) emission of dislocations from the sources, (ii) dislocations gliding on a slip plane until they are held up by an obstacle such as a grain boundary, and (iii) dislocations climbing out of their slip plane by vacancy emission. Following the stress drop an incubation period and negative creep were observed. The incubation time Δt appears as a consequence of the breakdown of the dynamic equilibrium between work hardening and dynamic recovery [14]. The presence or absence of an incubation period of zero creep in a stress reduction test can manifest whether

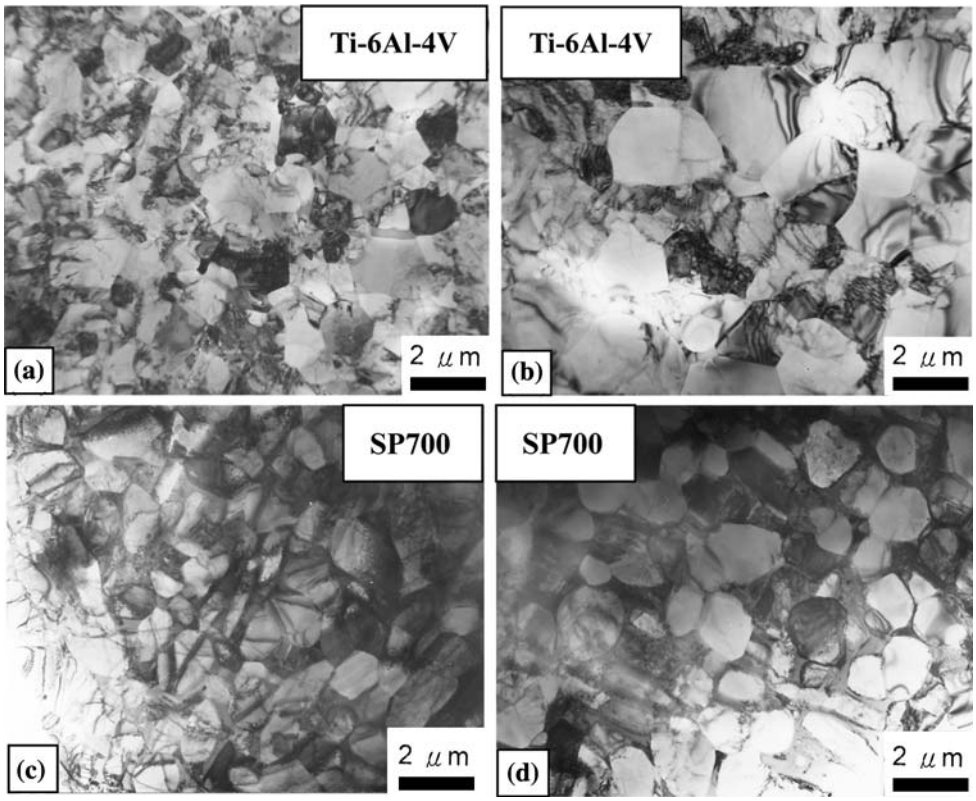

Fig. 4 TEM microstructure for the case of Ti–6–4 and SP700 at **a** and **c** 160 h creep; **b** and **d** 140 h creep followed by negative creep of 20 h after a stress drop

the mechanism of deformation is based on dislocation recovery within the incubation period, or on glide and climb without incubation [18]. The deformation structure in Fig. 4a, after 160 h creep of Ti–6–4 until the point of 5.5% strain, is compared with the structure of 140 h creep followed by negative creep 20 h after the stress drop, as depicted in Fig. 4b. The former exhibits a great number of dynamic recrystallized fine grains embedded and mixed with strained grains. The extent of the substructure formation is observed to increase with increased strain [18]. Nevertheless, in the latter specimen large dislocation-free grains appear surrounded by some small plastically deformed grains, which indicate that grain growth has occurred. The dislocations generated by deformation are rarely observed in α phase grains, whereas the β phase contains more dislocations in most grains. Also, consider the fact that the β phase has lower flow stress than the α phase at high temperatures [19]. It is apparent that most of the applied strains are accommodated by the soft β phase rather than by the hard α phase. The reason is that the β phase contains more dislocations due to the relatively fast accommodation process of applied strain. When the β phase accommodates most of the applied strains, the α phase does not experience much deformation, showing low density of dislocations in the α grains [19]. It is reasonable to assume that dislocations play an important role in creep. In contrast, the large and deformed elongated β grains occurring during creep in the alloy SP700 results in a better creep resistance, as shown in Fig. 2. There are many dynamically recrystallized fine subgrains in both specimens after 160 h of creep, as shown in Fig. 4a, c. Nevertheless, larger dislocation-free equiaxed subgrains have grown in the Ti–6–4 alloy compared to SP700 during negative creep as it becomes obvious in Fig. 4b, d. This microstructural variation is associated with the rate of dynamic dislocation recovery and grain growth, resulting in the creep rate and the dislocation density decrease after the anelastic response [20]. The observation of a different amount of negative creep/anelasticity on loading in Fig. 3 might be closely related to the difference in the amount of sub-grain coarsening in Fig. 4b, d namely the smaller negative creep/anelasticity rate for SP700 is associated with the slower dynamic subgrain growth.

Conclusion

This paper compares creep behaviors of two similar alloys. The creep resistance of the SP700 alloy with a larger grains size is superior to that of Ti–6–4 at 500 °C and an initial stress of 100 MPa, and exhibits a creep rate of only one-third of that of the latter alloy. The behavior of the stress drop leads to a negative creep for both titanium alloys. In the case of negative creep, the subgrains are obviously

larger than those occurring during constant creep, resulting from the fact that the new level of stress is lower than the internal stress for both titanium alloys. The dynamic recrystallized fine grains dispersed in the work hardened and deformed grains are attributed to the steady creep. The equiaxed coarse grains that exist after negative creep are caused by grain/subgrain growth. A smaller negative creep/anelasticity on loading for SP700 is closely associated to the slower grain/subgrain coarsening.

Acknowledgement This work was carried out with financial support from the National Science Council of the ROC, Taiwan, under the grants of NSC-94-2216-E-019-017 and NSC-95-2221-E-019-019. The authors gratefully acknowledge this support.

References

1. Leyens C, Peters M (2003) Titanium and titanium alloys fundamental and applications. Wiley-VCH Verlag, Weinheim, Germany, p 16
2. Collings EW (1994) Materials properties handbook: titanium alloys. ASM International, Materials Park, Ohio, p 488
3. Ouchi C, Minakawa K (1992) NKK Tech Rev 65:p61
4. Ouchi C, Fukai H (1999) Mat Sci Eng A 263:132
5. Ogawa A, Iizumi H (1996) Superplasticity and post-spf properties of SP-700. In: Proceedings of the conference Titanium '95: science and technology, vol I, Birmingham, UK, 22–26 October 1995, p 588
6. Takeda J, Niinomi M (2004) Int J Fatigue 26:1003
7. Barboza MJR, Moura Neto C (2004) Mat Sci Eng A 369:201
8. Seco FJ, Irisarri AM (2001) Fatigue Fract Eng M 24:741
9. Koike J, Maruyama K (1999) Mat Sci Eng A 263:155
10. Comley PN (2004) J Mater Eng Perform 13(6):660
11. Gunawarman A, Niinomi M (2001) Mater Sci Eng A 308:216
12. Barboza MJR, Moura Neto C, Silva CRM (2004) Mater Sci Eng A 369:201
13. Kruml T, Coddet O (2004) Mater Sci Eng A 387–389:72
14. Ahlquist CN, Nix WD (1971) Acta Metall 19:373
15. Lee HH (2008) The microstructure of high temperature deformation and welding residual stress analysis of titanium alloys. Master Thesis, National Taiwan Ocean University, Keelung, Taiwan, July
16. Es-Souni M (2001) Mater Charact 46(5):365
17. Poirier JP (1977) Acta Metall 25:913
18. Zhang WJ, Deevi SC (2002) Intermetallics 10:603
19. Kim JS, Kim JH (1999) Mat Sci Eng A 263:272
20. Blum W (2001) Mater Sci Eng A 319–321:8